Published by :
http://www.ijert.org

International Journal of Engineering Research & Technology (IJERT)
ISSN: 2278-0181
Vol. 14 Issue 06, June - 2025

Influence of Combining Different Infill Patterns on the Tensile and Flexural Strength of PLA Specimens

- Menna, G. Aboelella
PhD Student at the Design and Production Engineering Department, Faculty of Engineering, Ain Shams University, Cairo, Egypt.

- Samy, J. Ebeid
Professor at the Design and Production Engineering Department, Faculty of Engineering, Ain Shams University, Cairo, Egypt.

- Moustafa, M. Sayed
Professor at the Design and Production Engineering Department, Faculty of Engineering, Ain Shams University, Cairo, Egypt.

Abstract
This research addresses a critical gap in the understanding of Fused Deposition Modeling (FDM) by investigating the effects of hybrid infill configurations on the mechanical performance of Polylactic Acid (PLA) components. While the influence of individual infill patterns and densities on structural properties is well-documented, the synergistic effects of combining multiple pattern layers within a single part remain underexplored. This study systematically analyzes the tensile and flexural behavior of ASTM D638 Type-I and ASTM D790 specimens, respectively, fabricated with varying combinations of honeycomb, grid, and triangular infill patterns at 20% and 50% densities. The experimental results demonstrate that hybrid infill designs significantly enhance both tensile and flexural strength compared to single-pattern configurations. Notably, the combination of honeycomb and triangular patterns yielded a 58% increase in tensile strength, while a grid and triangular pattern combination resulted in a 53% improvement in flexural strength. By elucidating the fracture mechanisms associated with these hybrid configurations, this research provides valuable insights for optimizing FDM part design and enabling localized reinforcement in additive manufacturing applications.

Keywords: **Polylactic acid, Combined infill patterns, Polymer, 3D printing, Infill structure, Additive manufacturing, (FDM), tensile strength, flexural strength**

1. INTODUCTION

3D printing, or additive manufacturing, is increasingly recognized as a viable alternative to traditional subtractive processes, owing to its environmental benefits and machining advantages [1]. One of the primary advantages of 3D printing is minimal material loss and lower tool costs. Other advantages include simplified production equipment design, essentially no geometrical constraints, consistent raw materials (powder, filament, resin), and better material handling integration into modern manufacturing systems [2]. However, there are certain downsides to additive manufacturing technology. According to Attaran [3], the biggest disadvantage of 3D printing is that it is a relatively new technology with many unknown aspects.

The behavior of the material is studied after the printing process, especially when parameters such as printing, environmental conditions, etc. are not controlled. As a result, technology's dependability remains a concern. Studies have shown that layer thickness, infill percentage, and heat treatment are among the most important 3D printing settings [4], [5]. Other studies demonstrated how to increase the accuracy and efficiency of the Fused Deposition Modeling (FDM) process by optimizing the parameters [6],[7]. The air gap significantly impacts the wear strength of an FDM-fabricated component [8]. Other process parameters, such as building orientation [9], and raster angle [10], were also explored to see how they affected the performance of FDM printed parts. Raster width and the number of contours impact the mechanical performance of FDM-produced components [11]. Baich et al. [12] found that low density had comparable strength performance for tensile loading to high density. Onwubolu et al. showed that increasing layer and raster thickness improves the tensile strength of acrylonitrile butadiene styrene (ABS) [13]. However, Moradi et al [14]. indicated that layer thickness has a small impact on the mechanical capabilities of ABS material compared to other parameters. Dobos et al.[15] demonstrated empirically that assigning rasters longitudinally rather than diagonally results in the maximum tensile strength.

International Journal of Engineering Research & Technology (IJERT)
ISSN: 2278-0181
Vol. 14 Issue 06, June - 2025

There are also several research studies on modeling bending tests using appropriate pairings of 3D printing parameters to achieve better results. Gopsill et al. [16] investigated the stress variations generated in a bending test specimen. Initially, a static bending test was modeled using finite element analysis. The analysis's veracity was then verified by bending the real body. They performed a static bending test to optimize mechanical properties, which would be simulated in Ansys. Different filling patterns and reduced infill ratios enabled the weight and cost of the printed product to be reduced by 50% compared to the filled one. Today, thermoplastic surgical equipment can be produced via 3D printing. Load-bearing structures are designed to be stronger in areas where the most stress is applied.
Chacon et al. [17] conducted tensile and flexural tests to explore the effect of build orientation, feed rate, and layer thickness, and found that lower layer thickness and a higher feed rate resulted in optimal mechanical performance. The strongest orientation was on the edge, followed by flat, and the weakest was upright. Rajpurohit and Dave [18] confirmed that a 0° raster angle and reduced layer height result in higher tensile strength. Tensile strength increased with an increase in raster width up to a point and then dropped. Dave et al. [19] found that specimens with rectilinear and concentric infill patterns created in flat and long edge orientations had higher tensile strength than specimens with short edge orientations. They also reported that specimens with Hilbert curve infill patterns performed better for short-edge orientation than long-edge orientation. Rodriguez et al. [20] It was found that the presence of voids and loss of molecular orientation during extrusion reduced the strength of FDM samples compared to ABS monofilament.
Several methodologies have been utilized to explore the mechanical properties of FDM components, including FE simulations [21],[22],[23],[24], added fiber reinforcement in FDM parts[25],[26],[27],[28]. While studies have explored individual infill patterns and densities, this research introduces a novel approach by systematically investigating the combined effects of layered infill patterns in PLA. While extensive research has been conducted on the mechanical properties of 3D-printed parts with individual infill patterns, the potential of combining different patterns in a layered configuration remains largely unexplored. This study introduces a novel approach by systematically investigating the flexural and tensile behavior of 3D-printed specimens with layered hybrid infill structures. The novelty lies in examining the synergistic effects of combining distinct infill patterns across different layers, enabling the creation of parts with tailored mechanical properties. This approach offers the potential to optimize material usage, enhance structural performance, and develop new design guidelines for advanced 3D printing applications. Specifically, this research explores how layering infill patterns can create hybrid structures with enhanced or unique mechanical properties that cannot be achieved with single infill patterns, such as improved strength-to-weight ratios or direction-dependent stiffness."

2. METHODOLOGY

PLA was selected as the material for this investigation due to its favorable room-temperature mechanical properties, environmental sustainability, ease of processing, and superior print quality compared to traditional materials such as ABS and Nylon 6. A high-quality 1.75 mm PLA filament produced by Lancer 3D (Egypt) with a density of 1.24 g/cc [29] was employed. 3D printing was conducted on a ULTIMAKER S5 FDM 3D printer with dimensions of 330 x 240 x 300 mm, utilizing Ulti Maker Cura software for slicing and parameter optimization. Specifically, before printing the test specimens, a series of preliminary prints were conducted to optimize key parameters such as nozzle temperature, print speed, and layer height. These parameters were adjusted based on visual inspection and preliminary mechanical testing to achieve optimal print quality and minimize defects.

A. Design and manufacturing samples

To ensure adherence to ASTM D638 and D790 standards, tensile and flexural tests were conducted on 3D-printed specimens. The experimental design focused on investigating the influence of infill patterns and densities on the mechanical properties of PLA. Infill percentages of 20% and 50% were selected based on prior research indicating that these values represent critical thresholds for structural performance in FDM-printed components. Specifically, 20% infill is often used to minimize material consumption while maintaining structural integrity for non-load-bearing applications, whereas 50% infill provides a balance between strength and print time, suitable for moderately loaded parts. Due to equipment limitations preventing the direct creation of specimens with varying layer patterns, three distinct infill patterns—triangular, honeycomb, and grid—were designed using SolidWorks®.
These patterns, known for their distinct mechanical properties, were chosen for their respective strength characteristics, with triangular and honeycomb offering high strength-to-weight ratios and grid providing uniform support. The experimental design consisted of two primary specimen categories: single-layer and two-layer configurations. Single-layer specimens, printed directly from STL files without additional infill adjustments, featured either 20% or 50% infill density with one of the three selected patterns. To simulate multi-layer behavior and investigate the effects of combined infill patterns, two-layer specimens were designed in SolidWorks® due to the

International Journal of Engineering Research & Technology (IJERT)
ISSN: 2278-0181
Vol. 14 Issue 06, June - 2025

printer's inability to produce such configurations directly. These specimens consisted of two distinct layers, each featuring a different infill pattern (grid, triangle, or honeycomb) at either 20% or 50% infill density, as illustrated in Figures 2(a) and 2(b). This approach allowed for the examination of how combining different infill patterns at varying densities impacts tensile and flexural strength, as evaluated through ASTM D638 and D790 standards. The top and bottom layers were omitted during the printing of the two layer samples, as illustrated in Figure 1, to ensure the infill pattern was the focus of the testing.

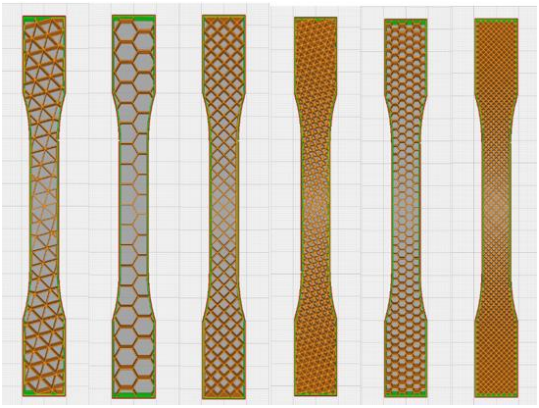

Figure 1. Single infill pattern samples for 20%& 50% infill

Figures 3 and 4 illustrate the fabricated specimens for the three design combinations (grid + triangle, grid + honeycomb, and honeycomb + triangle) at 20% and 50% infill densities, respectively. STL files for these three dissimilar pattern combinations were generated at 20% and 50% infill densities using SolidWorks® and subsequently imported into the 3D printing machine software for fabrication. To ensure statistical significance and accurate testing, six specimens were printed for each test (tensile and bending) in each category, with three replications per specimen, totaling 36 specimens. Data analysis will be based on the average values of these three replications.

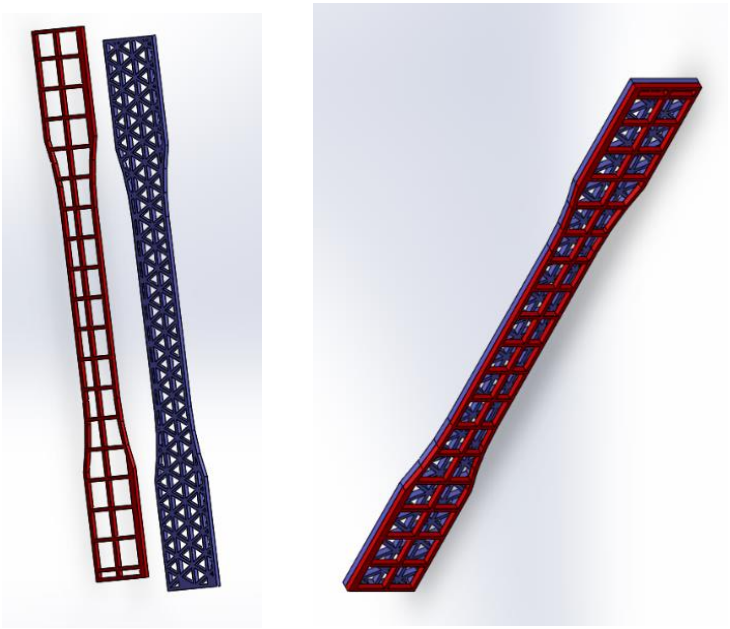

(a) (b)

Figure 2. Dissimilar patterns combination **a)** Two different patterns before combination **b)** Two different patterns after combination

International Journal of Engineering Research & Technology (IJERT)
ISSN: 2278-0181
Vol. 14 Issue 06, June - 2025

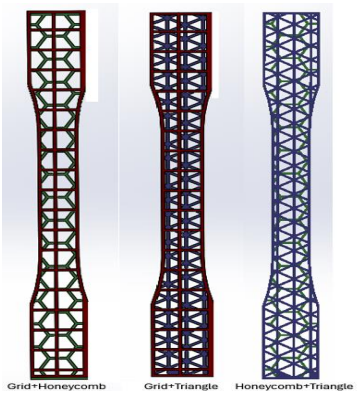

Figure 3. Dissimilar patterns combination 20% infill

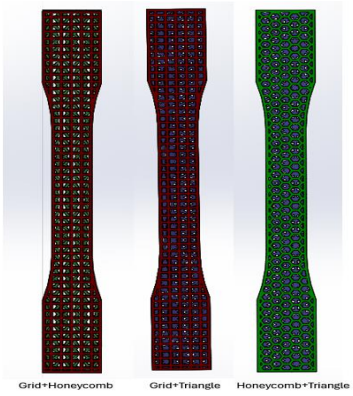

Figure 4. Dissimilar patterns combination 50% infill

Each experiment involved both fixed and variable parameters. Table 1 presents the key printing parameters used for the fabrication of PLA specimens. The initial layer height of 0.27mm represents the setup parameter defined in the Ulti maker Cura slicing software. This value was chosen to ensure adequate adhesion of the first layer to the build plate. The remaining layer height values were also set up parameters and set to 0.2mm. While these parameters were set up parameters, the actual layer height may have slight deviations due to the nature of the FDM process. The print speed of 60 mm/s was applied to all layers of the printed specimens. While it is common practice to reduce the print speed for the first layer to enhance adhesion, in this study, a consistent print speed of 60 mm/s was maintained throughout the printing process. This decision was made to maintain consistency across all specimens. The other parameters listed are also setup parameters that were input into the slicing software. The prepared specimens were printed to undergo tensile and bending tests. Table 2 provides a detailed description of the specimen codes and their corresponding characteristics.

B. Experimental setup (Tensile Strength Test)

Tensile strength tests were conducted on specimens conforming to ASTM D638 Type-I standards, with dimensions of 50 mm gauge length, 13 mm gauge width, and 5 mm thickness. To maintain a constant thickness of 5 mm, single-layer specimens utilized the full thickness for the infill pattern, while two-layer specimens allocated 2.5 mm to each layer. Figure 5 illustrates the 3D-printed specimens used in the tensile tests for both single-pattern and multi-pattern configurations. Tensile tests were performed on a computerized Universal Testing Machine with a 0.5-ton capacity at a controlled room temperature of 25.7°C ± 1°C. Specimens were positioned between the jaws of the testing machine with a grip distance of 115 mm, adhering to ASTM D638. The tests were conducted at a constant crosshead speed of 2 mm/min.At the end of each test, the strain percentage, ultimate tensile strength, and yield strength at break were recorded for each specimen.

Table 1 Fixed process parameters for FDM in 3D printing

Printing Parameters	Value
Nozzle diameter	0.4 mm
Initial layer height	0.27 mm
Infill line width	0.4 mm
Top/Bottom thickness	0 mm
Printing temperature	210◦C
Build plate temperature	55◦C
Print speed	60 mm/s

Table 2 Experimental specimen codes

Specimen Code	Description	Category	Infill Pattern	Infill Density (%)
S.T 20%	Single layer	1st category	Triangle	20%
S.H 20%	Single layer	1st category	Honeycomb	20%
S.G 20%	Single layer	1st category	Grid	20%
S.T 50%	Single layer	1st category	Triangle	50%
S.H 50%	Single layer	1st category	Honeycomb	50%
S.G 50%	Single layer	1st category	Grid	50%
D.T+G 20%	Two different layers	2nd category	Triangle+Grid	20%
D.G+H 20%	Two different layers	2nd category	Grid+Honeycomb	20%
D.H.C+T 20%	Two different layers	2nd category	Honeycomb+Triangle	20%
D.T+G 50%	Two different layers	2nd category	Triangle+Grid	50%
D.G+H 50%	Two different layers	2ndcategory	Grid+Honeycomb	50%
D.H.C+T 50%	Two different layers	2ndcategory	Honeycomb+Triangle	50%

Published by :
http://www.ijert.org

International Journal of Engineering Research & Technology (IJERT)
ISSN: 2278-0181
Vol. 14 Issue 06, June - 2025

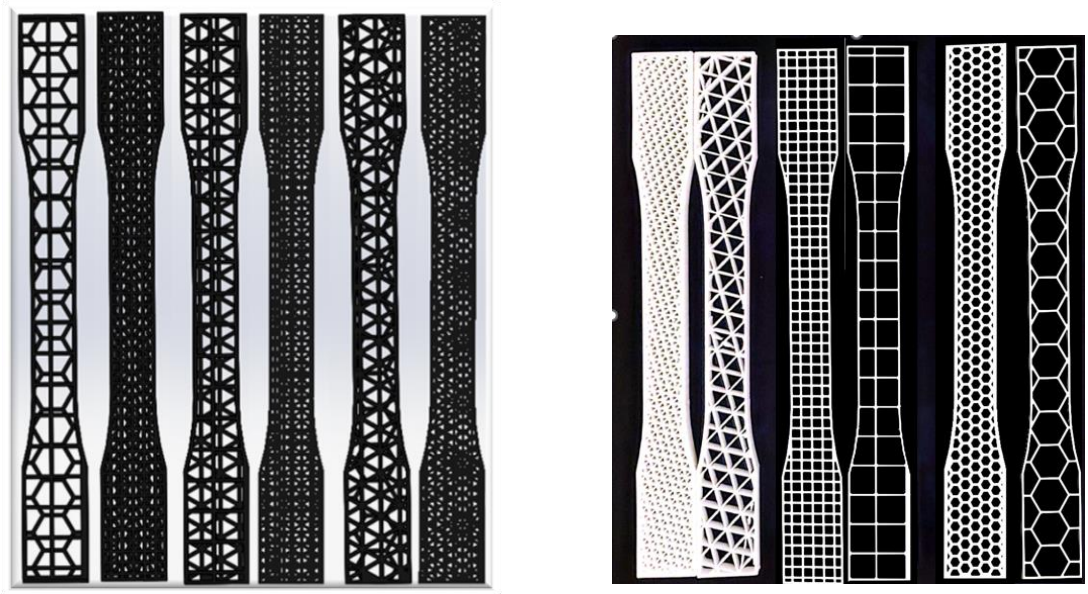

Figure 5. Tensile test specimens for 20% and 50% infill patterns **a)** single pattern specimens. **b)** different patterns combination specimens.

C. Experimental setup (Flexural Strength Test)

Flexural strength tests were conducted on specimens conforming to ASTM D790 standards, with dimensions of 70 mm gauge length, 15 mm gauge width, and 5 mm thickness. **Figures 6(a)** and **6(b)** illustrate the 3D-printed specimens used in the flexural strength tests.

The bending tests were performed on a computerized Universal Testing Machine with a 0.5-ton capacity at a controlled room temperature of 25.7°C ± 1°C. The specimens were tested until failure or reaching the equipment's limits

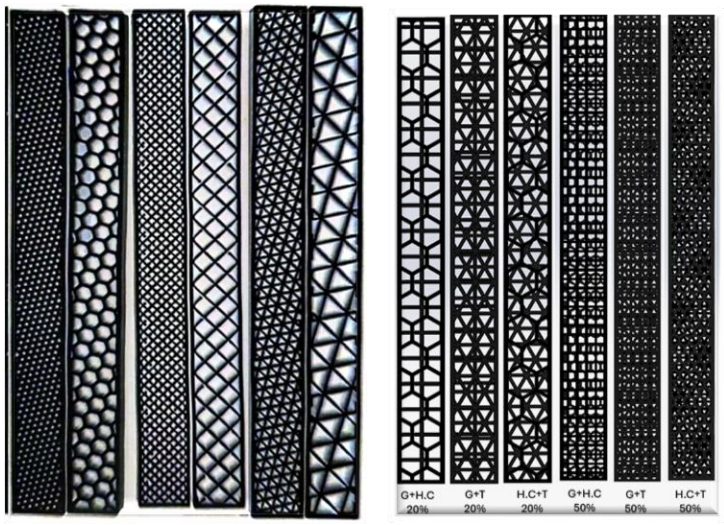

Figure 6. Flexural test specimens for 20% and 50% infill patterns **a)** single pattern specimens. **b)** different patterns combination specimens.

3. RESULTS AND DISCUSSION

A. Tensile test results

Stress-strain curves for the 3D-printed specimens are presented in Figure 7. A comparative analysis of various pattern combinations and single-layer patterns is depicted in Figure 8.

Published by :
http://www.ijert.org

International Journal of Engineering Research & Technology (IJERT)
ISSN: 2278-0181
Vol. 14 Issue 06, June - 2025

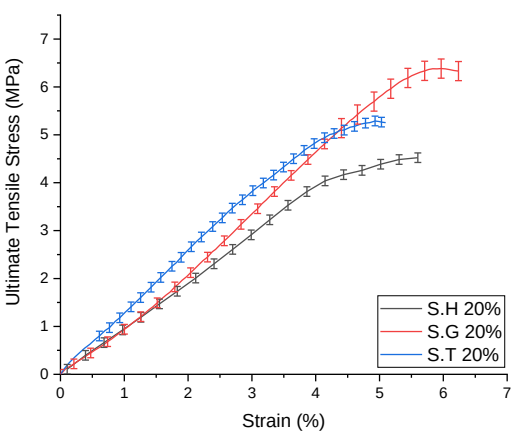

(a)

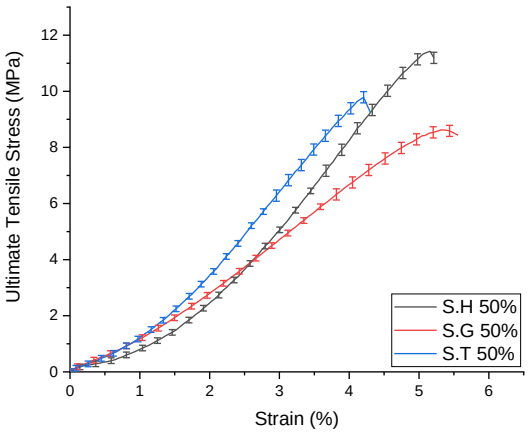

(b)

IJERTV14IS060045

Published by :
http://www.ijert.org

International Journal of Engineering Research & Technology (IJERT)
ISSN: 2278-0181
Vol. 14 Issue 06, June - 2025

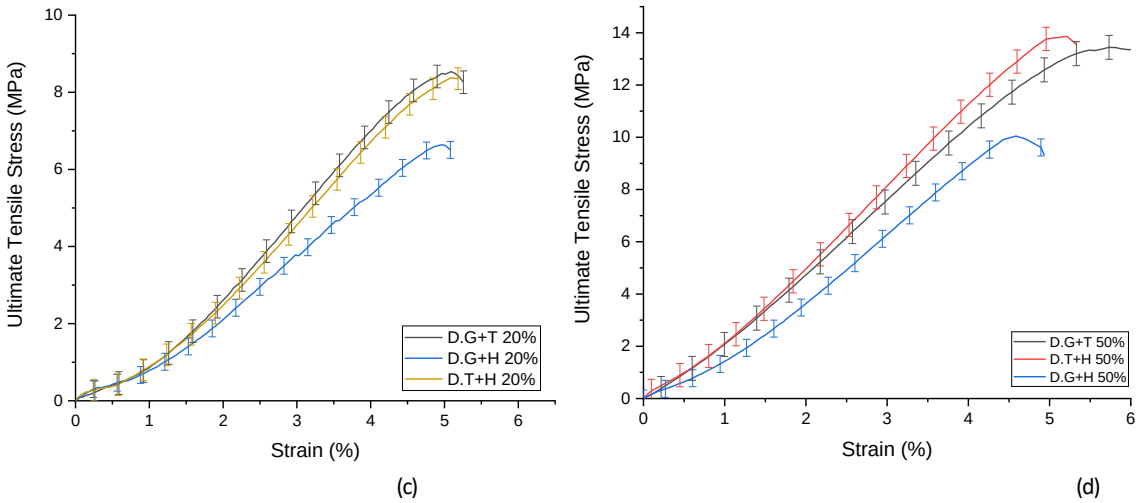

Figure 7. Stress-strain curve for prepared specimens **a)** Single layer at 20% infill **b)** Single layer at 50% infill **c)** Different combined patterns at 20% infill **d)** Different combined patterns at 20% infill

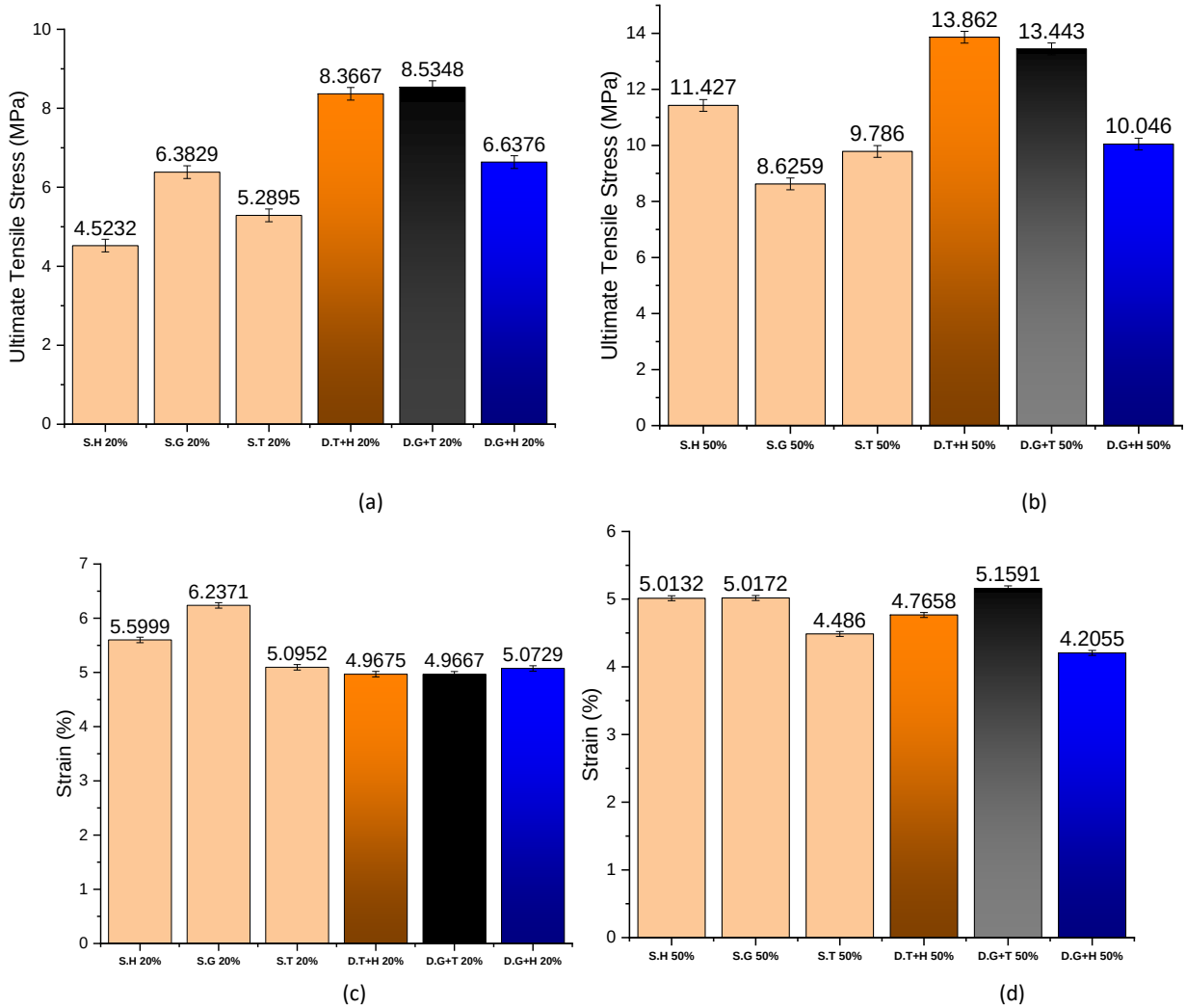

Figure 8. A comparison between different prepared specimens **a)** Ultimate strength for 20% infill **b)** Ultimate strength for 50% infill **c)** Strain percentage for 20% infill **d)** Strain percentage for 50% infill

International Journal of Engineering Research & Technology (IJERT)
ISSN: 2278-0181
Vol. 14 Issue 06, June - 2025

Figure 7(a) demonstrates that at a 20% infill density, combining the honeycomb pattern with triangular patterns leads to a significant enhancement in tensile strength compared to the standalone honeycomb pattern. A similar trend is observed when the honeycomb pattern is combined with the grid pattern, although the improvement is less pronounced. Additionally, the combination of grid and triangular patterns results in a higher tensile strength than the grid pattern alone. However, combining grid and honeycomb patterns exhibits a negligible impact on tensile strength compared to the standalone grid pattern. Combining patterns at a 50% infill density demonstrates a behavior consistent with that observed for patterns at a 20% infill density.

As observed in Figures 7(b) and 8, increasing infill density correlates with a decrease in void volume, leading to a subsequent enhancement in tensile strength. This trend is particularly evident in the triangular plus honeycomb combined pattern, where the lowest tensile strength occurs at 20% density, while the highest value of 13.86 MPa is achieved at 50% density. A direct correlation was observed between infill density and material consumption. Samples with infill densities of 20% and 50% exhibited masses of 9g and 12g, respectively, indicating a 33% increase in material usage. While a 50% infill density maximizes strength, it adversely impacts overall cost due to increased printing time and material consumption.

A consistent increase in tensile strength is observed across all three different combined infill patterns, suggesting a similar underlying mechanism. This behavior can be attributed to the ability of the infill fibers to deform and dissipate stress. As density increases, this deformation capacity is amplified, contributing to higher tensile strength.

B. Flexural test results

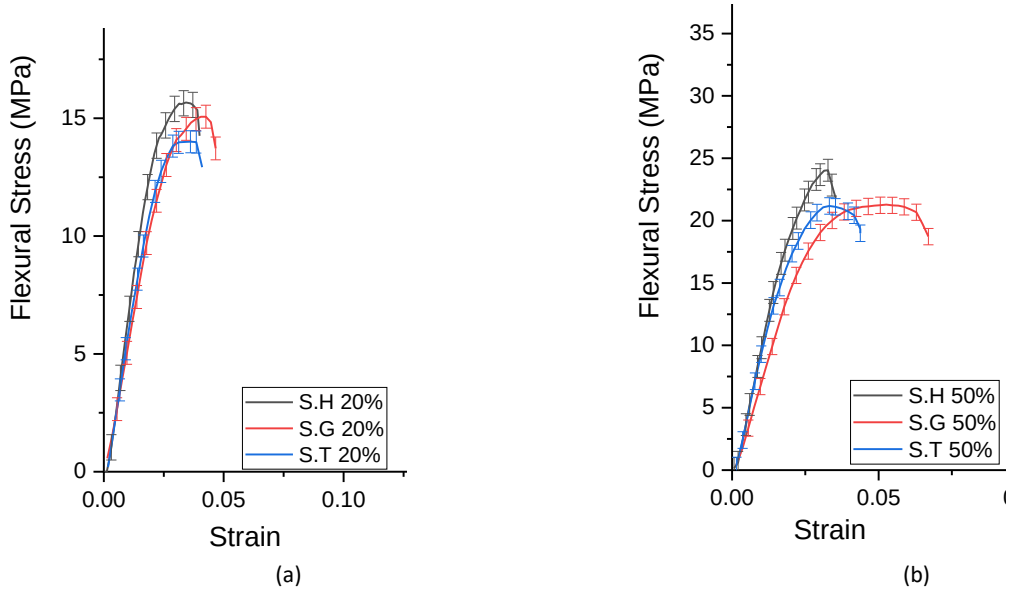

Published by :
http://www.ijert.org

International Journal of Engineering Research & Technology (IJERT)
ISSN: 2278-0181
Vol. 14 Issue 06, June - 2025

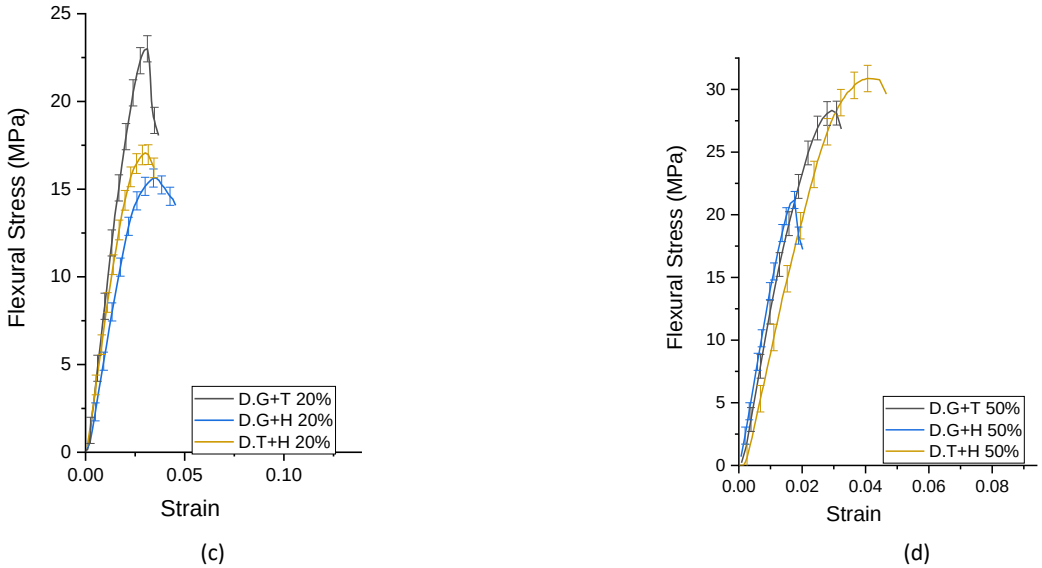

Figure 9. Stress-strain curve for prepared specimens **a)** Single layer at 20% infill **b)** Single layer at 50% infill **c)** Different combined patterns at 20% infill **d)** Different combined patterns at 20% infill

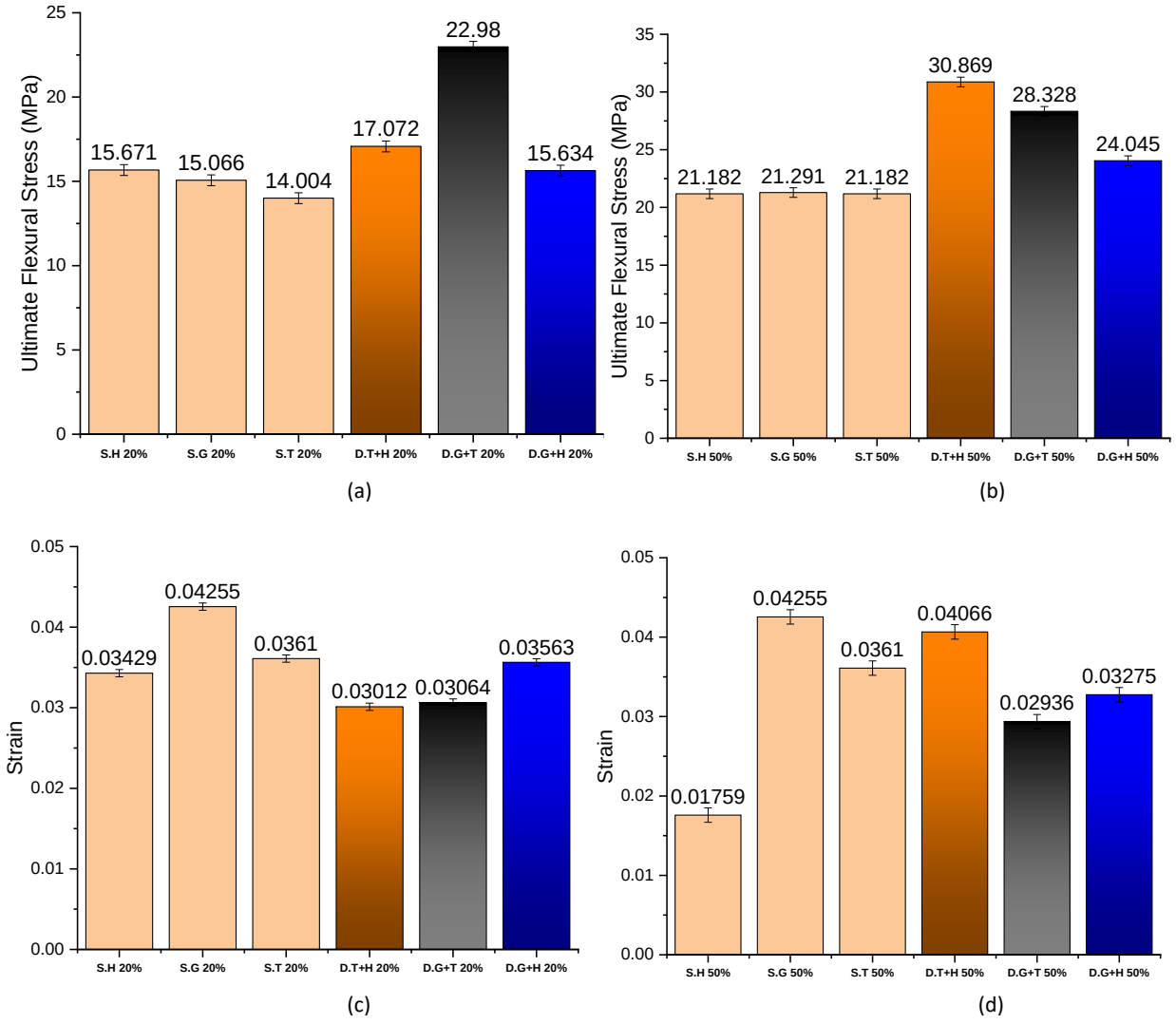

IJERTV14IS060045

International Journal of Engineering Research & Technology (IJERT)
ISSN: 2278-0181
Vol. 14 Issue 06, June - 2025

Figure 10. A comparison between different prepared specimens a) Ultimate strength for 20% infill b) Ultimate strength for 50% infill c) Strain percentage for 20% infill d) Strain percentage for 50% infill

As depicted in Figure 9(a), a significant enhancement in flexural strength was observed when a honeycomb pattern was combined with triangular patterns at a 20% infill density, reaching a maximum value of 22.98 MPa, compared to the standalone honeycomb pattern. A similar trend was noted for the combination of grid and honeycomb patterns, albeit with a less pronounced improvement. Furthermore, the hybrid configuration of the grid and triangular patterns exhibited a higher flexural strength than the grid and the triangular pattern alone.

This trend persisted at a 50% infill density, as illustrated in Figures 9(b) and 10. As discussed in the tensile test section, the increased flexural strength at the 50% infill density can be attributed to the reasons discussed previously in the tensile test results.

4. FRACTURE ANALYSIS OF COMBINED INFILL PATTERN

A. Tensile test analysis

A comprehensive analysis of the tensile resistance of each infill density and pattern combination was conducted to evaluate their impact on crack initiation, propagation, and overall tensile strength.

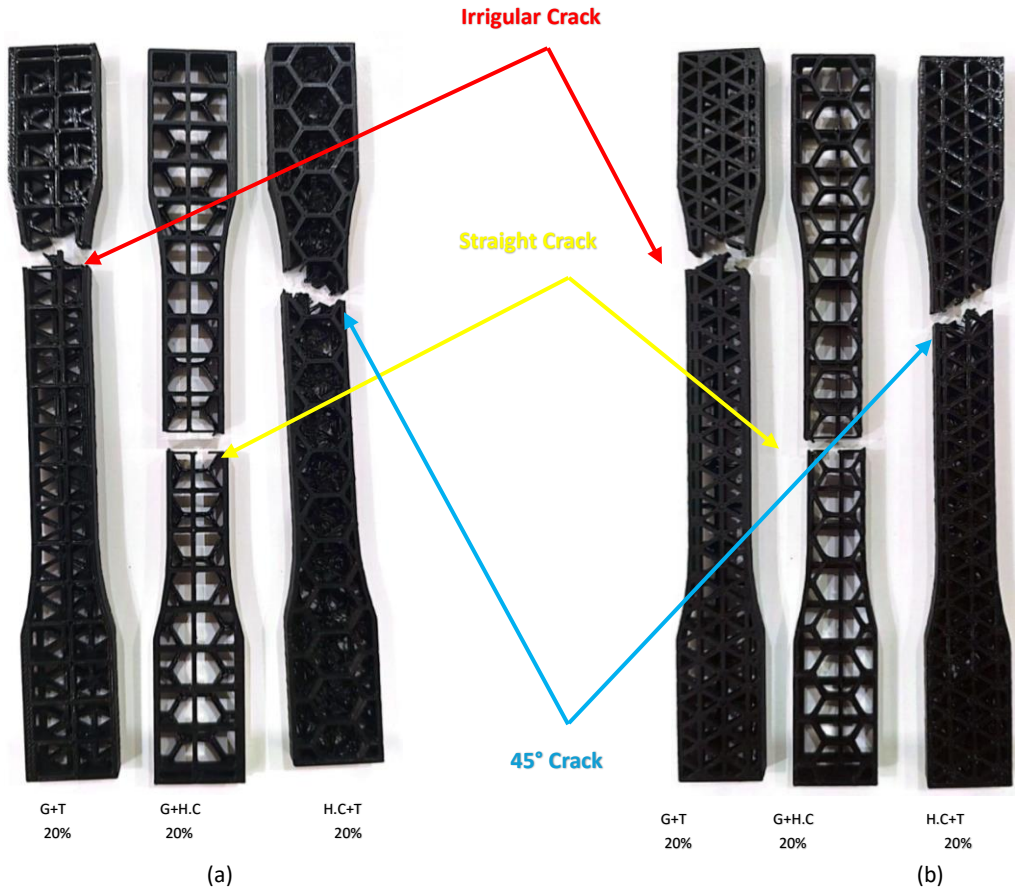

Published by :
http://www.ijert.org

International Journal of Engineering Research & Technology (IJERT)
ISSN: 2278-0181
Vol. 14 Issue 06, June - 2025

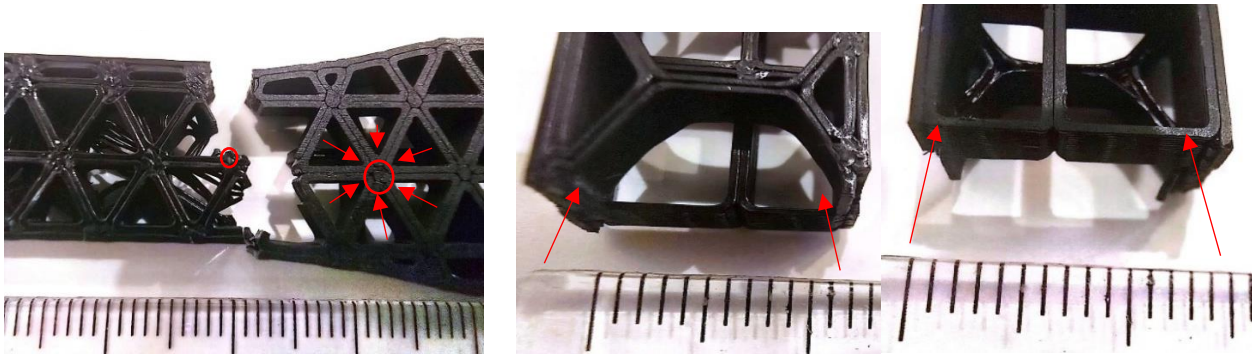

(c) (d) (e)

Figure 11. Tensile specimen fracture at 20% infill density **a)** front of Specimen **b)** back of specimen **c)** Triangle pattern fracture **d)** honeycomb pattern fracture **e)** grid pattern fracture.

Figure 11 illustrates the fracture mechanisms observed in 20% of infill density specimens.

(Grid+Triangle) This configuration exhibited an irregular crack propagation pattern, primarily following the beads of the triangular pattern. This suggests that the sharp angles of the triangular pattern act as stress concentrators, weakening the overall structure and leading to localized failure. **(Honeycomb+Grid)** In contrast, a straight crack propagated directly between the honeycomb and grid patterns. This indicates a clear point of weakness where stress concentrates due to the alignment of the beads from both patterns. **(Honeycomb+Triangle)** This configuration demonstrated a 45-degree angled crack, again following the triangular patterns beads. While the triangular pattern offers inherent strength, its sharp angles still induce stress concentration. However, the combination with the honeycomb pattern allows for a more effective distribution of stress compared to the other two configurations.

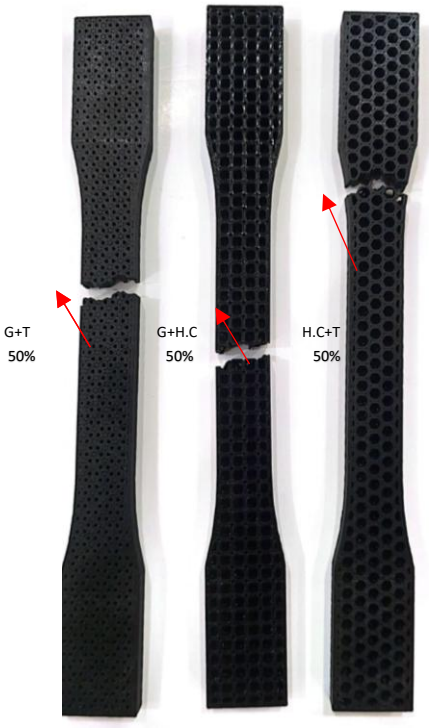

Figure 12. Tensile specimen fracture at 50% infill density

As illustrated in Figure 11(c), the sharp intersections of the beads of the triangular patterns serve as stress concentration points, initiating and propagating cracks at these locations. This phenomenon is evident in the two pattern combinations incorporating the triangular pattern, where fractures predominantly follow the beads of the triangular pattern. In contrast, Figures. 11(d) and (e) depict fracture within the honeycomb and grid patterns, respectively, in the (Honeycomb+Grid) combination. Figure 12 illustrates the fracture behavior of 50% infill combinations, showcasing smooth and continuous fracture patterns. The (Triangle+Honeycomb) and (Triangle+Grid) specimens exhibited fractures following the stress concentrations induced by the triangular pattern, as previously discussed. The (Honeycomb+Grid) specimen demonstrated a fracture pattern similar to that observed in the 20% infill density

International Journal of Engineering Research & Technology (IJERT)
ISSN: 2278-0181
Vol. 14 Issue 06, June - 2025

The triangular pattern, despite its strength, is susceptible to stress concentration due to its sharp angles. The honeycomb pattern, with its obtuse angles, provides superior stress distribution. The grid pattern offers a balance between strength and stress distribution but can be less effective when combined with patterns that induce high-stress concentrations. To optimize the mechanical performance of 3D printed parts, designers should carefully consider the specific application and select infill patterns that balance strength and stress distribution while minimizing sharp angles.

B. Flexural test analysis

A comprehensive analysis of the flexural resistance for each infill density and pattern combination was conducted to evaluate their influence on crack propagation and, subsequently, the specimen's flexural strength capabilities. As observed, during bending tests, fractures consistently initiate at the bottom layer of the specimen, where maximum tensile stress is concentrated. Therefore, careful consideration must be given to the layer orientation when constructing multi-different layered objects subjected to bending stress.

Figure 13. Flexural strength specimen fractures **a)** at 20% infill density, **b)** at 50% infill density **c)** fracture at grid pattern **d)** bending of honeycomb pattern **e)** fracture at triangle pattern

Figure 13 presents the fracture analysis of flexural test specimens with the two different infill densities (20% and 50%). In **Figure 13(a)** at the 20% infill, it can be shown that.

International Journal of Engineering Research & Technology (IJERT)
ISSN: 2278-0181
Vol. 14 Issue 06, June - 2025

Grid+Honeycomb: In this configuration, crack initiation and propagation were predominantly observed within the triangular pattern, while the honeycomb pattern exhibited only deformation. This suggests that the sharp angles of the triangular pattern act as stress concentrators, leading to localized failure. (Triangle+honeycomb) Similarly, cracks were confined to the triangular pattern, highlighting their susceptibility to flexural stress. The honeycomb pattern, characterized by its obtuse angles, demonstrated superior resistance to deformation. (Grid+Triangle) In this configuration, the grid pattern exhibited initial crack formation, followed by secondary cracking in the triangular pattern. This indicates that the grid pattern is less resistant to flexural stress than the triangular pattern.
Based on the observed fracture patterns, it can be inferred that the honeycomb pattern possesses the highest flexural strength, followed by the triangular pattern and subsequently the grid pattern. Combining the honeycomb pattern with the grid or triangular pattern enhances flexural strength and ductility. This improvement is likely attributed to the synergistic effect of the combined patterns, which facilitates a more efficient distribution of stress and energy dissipation. Figure 13(b) illustrates that at a 50% infill density, all three pattern combinations exhibited ductile behavior, undergoing significant plastic deformation without experiencing complete fracture. This suggests an enhanced ability to absorb flexural energy through plastic deformation rather than brittle failure. This ductile behavior can be attributed to the increased infill density, as previously discussed in the context of Figures 7(b) and 8. Figure 13(c) and (e) illustrate the fracture mechanisms of the triangular and grid patterns, respectively, which align with the fracture behavior observed in the previous tensile test results. In contrast, Figure 13(d) demonstrates the ductile behavior of the honeycomb pattern, which exhibited significant bending deformation without fracturing.

5.CONCLUSION

This study demonstrates the significant impact of combining different infill patterns on the tensile and flexural strength of 3D-printed PLA specimens. By strategically combining patterns, it is possible to enhance the mechanical properties of 3D-printed parts and optimize their performance for specific applications. The combination of different infill patterns, as previously discussed, resulted in enhanced tensile and flexural strength for both 20% and 50% infill densities. Increasing infill density to 50% correlates with a decrease in void volume, leading to a subsequent enhancement in tensile and flexural strength. However, careful consideration must be given to the layer location, whether at the top or bottom, particularly when constructing multi-layered objects composed of different patterns and subjected to bending stress.

Honeycomb pattern: The combination of honeycomb and triangular patterns yielded a significant enhancement in both tensile and flexural strength compared to the standalone honeycomb. While the combination of honeycomb and grid patterns resulted in a slight improvement in both properties, the effect on flexural strength was negligible. The honeycomb pattern, with its obtuse angles, provides superior stress distribution

Triangular pattern: Combining a triangular pattern with a grid pattern resulted in increased tensile and flexural strength compared to the standalone triangular pattern. However, this enhancement was less significant than when combining the triangular and honeycomb patterns. Despite its inherent strength, the susceptibility of the triangular pattern to stress concentration is due to its sharp angles.

Grid pattern: The grid pattern offers a balance between strength and stress distribution. However, its effectiveness diminishes when combined with patterns that induce high-stress concentrations, such as the triangular pattern. Furthermore, its negligible impact on the flexural strength of the honeycomb pattern, particularly at low infill densities (20%), is evident. However, at higher infill densities (50%), the grid pattern exhibits improved strength and compatibility with other patterns

The current study provides valuable insights for both design and production engineers, enabling them to optimize the strength-to-weight ratio of 3D printed parts through material reduction. Additionally, the information on the layer combination can aid designers in selecting the most suitable 3D printing parameters for their specific applications. To optimize the mechanical performance of 3D printed parts, designers should carefully consider the specific application and select infill patterns that balance strength and stress distribution while minimizing sharp angles. Further research is needed to explore the effects of other infill patterns, layer orientation, and different materials on the mechanical behavior of 3D printed structures.

International Journal of Engineering Research & Technology (IJERT)
ISSN: 2278-0181
Vol. 14 Issue 06, June - 2025

6. ACKNOWLEDGMENT

I truly thank my supervisor for helping me and giving useful advice during this research. I am also very thankful to my family and well-wishers for their support, good suggestions, and encouragement. Most importantly, I thank God for giving me the strength and guidance to complete this work successfully.

REFRANCES

[1] B. Baz, G. Aouad, and S. Remond, "Effect of the printing method and mortar's workability on pull-out strength of 3D printed elements," Constr. Build. Mater., vol. 230, p. 117002, Jan. 2020, doi: 10.1016/J.CONBUILDMAT.2019.117002.

[2] T. D. Ngo, A. Kashani, G. Imbalzano, K. T. Q. Nguyen, and D. Hui, "Additive manufacturing (3D printing): A review of materials, methods, applications and challenges," Compos. Part B Eng., vol. 143, pp. 172–196, Jun. 2018, doi: 10.1016/J.COMPOSITESB.2018.02.012.

[3] M. Attaran, "The rise of 3-D printing: The advantages of additive manufacturing over traditional manufacturing," Bus. Horiz., vol. 60, no. 5, pp. 677–688, Sep. 2017, doi: 10.1016/J.BUSHOR.2017.05.011.

[4] J. Torres, J. Cotelo, J. Karl, and A. P. Gordon, "Mechanical property optimization of FDM PLA in shear with multiple objectives," JOM, vol. 67, no. 5, pp. 1183–1193, May 2015, doi: 10.1007/S11837-015-1367-Y/TABLES/4.

[5] M. M. Hanon, R. Marczis, and L. Zsidai, "Anisotropy Evaluation of Different Raster Directions, Spatial Orientations, and Fill Percentage of 3D Printed PETG Tensile Test Specimens," Key Eng. Mater., vol. 821, pp. 167–173, 2019, doi: 10.4028/WWW.SCIENTIFIC.NET/KEM.821.167.

[6] P. Geng et al., "Effects of extrusion speed and printing speed on the 3D printing stability of extruded PEEK filament," J. Manuf. Process., vol. 37, pp. 266–273, Jan. 2019, doi: 10.1016/J.JMAPRO.2018.11.023.

[7] W. Wu, P. Geng, G. Li, D. Zhao, H. Zhang, and J. Zhao, "Influence of layer thickness and raster angle on the mechanical properties of 3D-printed PEEK and a comparative mechanical study between PEEK and ABS," Materials (Basel)., vol. 8, no. 9, pp. 5834–5846, 2015, doi: 10.3390/MA8095271.

[8] V. Vijayaraghavan, A. Garg, J. S. L. Lam, B. Panda, and S. S. Mahapatra, "Process characterisation of 3D-printed FDM components using improved evolutionary computational approach," Int. J. Adv. Manuf. Technol., vol. 78, no. 5–8, pp. 781–793, May 2015, doi: 10.1007/S00170-014-6679-5/METRICS.

[9] G. Alaimo, S. Marconi, L. Costato, and F. Auricchio, "Influence of meso-structure and chemical composition on FDM 3D-printed parts," Compos. Part B Eng., vol. 113, pp. 371–380, Mar. 2017, doi: 10.1016/J.COMPOSITESB.2017.01.019.

[10] M. R. Ayatollahi, A. Nabavi-Kivi, B. Bahrami, M. Yazid Yahya, and M. R. Khosravani, "The influence of in-plane raster angle on tensile and fracture strengths of 3D-printed PLA specimens," Eng. Fract. Mech., vol. 237, p. 107225, Oct. 2020, doi: 10.1016/J.ENGFRACMECH.2020.107225.

[11] A. W. Gebisa and H. G. Lemu, "Influence of 3D Printing FDM Process Parameters on Tensile Property of ULTEM 9085," Procedia Manuf., vol. 30, pp. 331–338, Jan. 2019, doi: 10.1016/J.PROMFG.2019.02.047.

[12] L. Baich, G. Manogharan, and H. Marie, "Study of infill print design on production cost-time of 3D printed ABS parts," Int. J. Rapid Manuf., vol. 5, no. 3/4, p. 308, 2015, doi: 10.1504/IJRAPIDM.2015.074809.

[13] G. C. Onwubolu and F. Rayegani, "Characterization and Optimization of Mechanical Properties of ABS Parts Manufactured by the Fused Deposition Modelling Process," Int. J. Manuf. Eng., vol. 2014, no. 1, p. 598531, Jan. 2014, doi: 10.1155/2014/598531.

[14] M. Moradi, R. Hashemi, and M. Kasaeian-Naeini, "Experimental investigation of parameters in fused filament fabrication 3D printing process of ABS plus using response surface methodology," Int. J. Adv. Manuf. Technol., pp. 1–18, May 2023, doi: 10.1007/S00170-023-11468-0/FIGURES/14.

[15] J. Dobos, M. M. Hanon, and I. Oldal, "Effect of infill density and pattern on the specific load capacity of FDM 3D-printed PLA multi-layer sandwich," J. Polym. Eng., vol. 42, no. 2, pp. 118–128, Feb. 2022, doi: 10.1515/POLYENG-2021-0223/MACHINEREADABLECITATION/RIS.

[16] J. A. Gopsill, J. Shindler, and B. J. Hicks, "Using finite element analysis to influence the infill design of fused deposition modelled parts," Prog. Addit. Manuf., vol. 3, no. 3, pp. 145–163, Sep. 2018, doi: 10.1007/S40964-017-0034-Y/FIGURES/20.

[17] J. M. Chacón, M. A. Caminero, E. García-Plaza, and P. J. Núñez, "Additive manufacturing of PLA structures using fused deposition modelling: Effect of process parameters on mechanical properties and their optimal selection," Mater. Des., vol. 124, pp. 143–157, Jun. 2017, doi: 10.1016/J.MATDES.2017.03.065.

[18] H. K. Dave, B. H. Patel, S. R. Rajpurohit, A. R. Prajapati, and D. Nedelcu, "Effect of multi-infill patterns on tensile behavior of FDM printed parts," J. Brazilian Soc. Mech. Sci. Eng., vol. 43, no. 1, pp. 1–15, Jan. 2021, doi: 10.1007/S40430-020-02742-3/FIGURES/22.

[19] H. K. Dave, N. H. Patadiya, A. R. Prajapati, and S. R. Rajpurohit, "Effect of infill pattern and infill density at varying part orientation on tensile properties of fused deposition modeling-printed poly-lactic acid part," Proc. Inst. Mech. Eng. Part C J. Mech. Eng. Sci., vol. 235, no. 10, pp. 1811–1827, May 2021, doi: 10.1177/0954406219856383/ASSET/IMAGES/LARGE/10.1177_0954406219856383-FIG18.JPEG.

[20] J. F. Rodríguez, J. P. Thomas, and J. E. Renaud, "Mechanical behavior of acrylonitrile butadiene styrene fused deposition materials modeling," Rapid Prototyp. J., vol. 9, no. 4, pp. 219–230, 2003, doi: 10.1108/13552540310489604/FULL/PDF.

[21] D. W. Abbot, D. V. V. Kallon, C. Anghel, and P. Dube, "Finite Element Analysis of 3D Printed Model via Compression Tests," Procedia Manuf., vol. 35, pp. 164–173, Jan. 2019, doi: 10.1016/J.PROMFG.2019.06.001.

[22] S. D. Shelare, K. R. Aglawe, and P. B. Khope, "Computer aided modeling and finite element analysis of 3-D printed drone," Mater. Today Proc., vol. 47, pp. 3375–3379, Jan. 2021, doi: 10.1016/J.MATPR.2021.07.162.

[23] R. Jerez-Mesa, J. A. Travieso-Rodriguez, X. Corbella, R. Busqué, and G. Gomez-Gras, "Finite element analysis of the thermal behavior of a RepRap 3D printer liquefier," Mechatronics, vol. 36, pp. 119–126, Jun. 2016, doi: 10.1016/J.MECHATRONICS.2016.04.007.

[24] D. Calneryte et al., "Multi-scale finite element modeling of 3D printed structures subjected to mechanical loads," Rapid Prototyp. J., vol. 24, no. 1, pp. 177–187, 2018, doi: 10.1108/RPJ-05-2016-0074/FULL/PDF.

[25] S. Christ, M. Schnabel, E. Vorndran, J. Groll, and U. Gbureck, "Fiber reinforcement during 3D printing," Mater. Lett., vol. 139, pp. 165–168, Jan. 2015, doi: 10.1016/J.MATLET.2014.10.065.

International Journal of Engineering Research & Technology (IJERT)
ISSN: 2278-0181
Vol. 14 Issue 06, June - 2025

[26] N. van de Werken, J. Hurley, P. Khanbolouki, A. N. Sarvestani, A. Y. Tamijani, and M. Tehrani, "Design considerations and modeling of fiber reinforced 3D printed parts," Compos. Part B Eng., vol. 160, pp. 684–692, Mar. 2019, doi: 10.1016/J.COMPOSITESB.2018.12.094.

[27] K. I. Ismail, T. C. Yap, and R. Ahmed, "3D-Printed Fiber-Reinforced Polymer Composites by Fused Deposition Modelling (FDM): Fiber Length and Fiber Implementation Techniques," Polym. 2022, Vol. 14, Page 4659, vol. 14, no. 21, p. 4659, Nov. 2022, doi: 10.3390/POLYM14214659.

[28] B. Akhoundi, A. H. Behravesh, and A. Bagheri Saed, "Improving mechanical properties of continuous fiber-reinforced thermoplastic composites produced by FDM 3D printer," J. Reinf. Plast. Compos., vol. 38, no. 3, pp. 99–116, Feb. 2019, doi: 10.1177/0731684418807300/ASSET/IMAGES/LARGE/10.1177_0731684418807300-FIG20.JPEG.

[29] "Ultimate 3D Printing Material Properties Table." Accessed: Aug. 15, 2024. [Online]. Available: https://www.simplify3d.com/resources/materials-guide/properties-table/